Mem. S.A.It. Vol. 95, 11

Memorie della

The PLanet extreme Ultraviolet Spectrometer

A. Meneguzzo[1], M. Bazzan[2], M. Carminati[3], A.J. Corso[1], E. Fabbrica[3], G. Favaro[2], C. Fiorini[3], M. Fiorini[4], S. Incorvaia[4], L. Nassi[3], G. Maggioni[2], M. Padovani[5], M.G. Pelizzo[1,5], L. Schettini[4], G. Toso[4], and M. Uslenghi[4]

[1] Consiglio Nazionale delle Ricerche - Istituto di Fotonica e Nanotecnologie (CNR-IFN), via Trasea, 7,35131 Padova, Italy
[2] Università di Padova, Dipartimento di Fisica e Astronomia, via Marzolo 8, 35131 Padova, Italy
[3] Politecnico di Milano, Dipartimento di Elettronica, Informazione e Bioingegneria, and INFN Sezione di Milano, Milano, Italy
[4] Istituto Nazionale di Astrofisica, Istituto di Astrofisica e Fisica Cosmica Milano, Via A. Corti 12, 20133 Milano, Italy

Received: 26 March 2024; Accepted: 1 July 2024

Abstract.
Spectroscopic observations in the far ultraviolet (FUV, 115-200 nm) and extreme ultraviolet (EUV, 50-120 nm) are of great interest in many astronomical fields, such as solar physics, interstellar medium physics, and planetary sciences. In particular, FUV/EUV spectroscopy is the main technique for studying planetary exospheres but is of significant importance also for geological studies, water ice research, analysis of dust systems, and of aurora phenomena. The development of FUV/EUV spectrometers is crucial for the upcoming planetary exploration missions. This work is focused on the PLanetary Ultraviolet Spectrometer (PLUS), a project funded by the Italian Space Agency (ASI). PLUS has the aim to develop the technology needed for a new generation of FUV/EUV spectrometers, having higher spatial and spectral resolution, improved detection limits, shorter observation integration time, and higher dynamic range with respect the past instrumentation. Such characteristics are obtained by the combination two key technologies: optical components optimized for each channel, combined with an high resolution/dynamic range solar-blind photon counting detectors. The photon counting detector will be based on a Micro-Channel Plate (MCP) coupled with an application-specific integrated Circuit (ASIC) read-out system.

Key words. EUV/FUV spectroscopy, exosphere, ice research, EUV/FUV albedo, MCP, ASIC readout system

1. Introduction

Space missions equipped with spectroscopic instruments operating in the extreme ultraviolet (EUV, $\lambda = 50 - 120$ nm) and in the far ultraviolet (FUV, $\lambda = 120 - 300$ nm) play a fundamental role in various scientific fields, such as in solar and interstellar medium physics, and in the study of planets and minor bodies. In planetology, these spectral ranges

are particularly suitable for investigating planetary and minor body exospheres in terms of their dynamics and chemical composition. However, they can also provide a valuable contribution to the determination of the surface composition of rocky bodies, to the research of water ice on permanently shielded craters, and to the study of aurora phenomena occurring in planets having active magnetospheres (Hendrix et al., 2020).

In the study of planetary exospheres and in the detection of volatile components around comets and asteroids, EUV/FUV spectroscopic observations allow to acquire the spectral signatures of many constituents, including neutral atoms and their relative ions (N, H, He, C, O, S, ...) hydrocarbons (CH_4, C_2H_4, ...) and molecules (H_2O, HO, S_2O, ...) (Hörst, 2017; Stevens et al., 2015). For example, New Horizons/Alice was able to observe Pluto's upper atmosphere and detected the emission of H, N, CO, methylacetylene, and Ar (Gladstone et al., 2016). Combined observations of the spectrometers LRO/LAMP (Gladstone et al., 2005) and LADEE/UVS (Elphic et al., 2015) detected many different species in the lunar exosphere, including H, He, Ar, CH_4, N_2, CO, CO_2, O, Na e K and likely Mg, Ca, Fe, Si, OH, Xe, Kr, S. Recently, BepiColobo/PHEBUS investigated the profile of the He Mercury' exosphere during the second fly-by of the mission (Quémerais et al., 2023). Rosetta/Alice, which observed the 67P/C-G comet for two years, detected many signatures of volatile components, including H_2O, CO, CO_2, whose abundances were then correlated with the comet activity. The instrument has also monitored the expelled ice, and the interaction between the coma and Coronal Mass Ejections (CMEs), improving the understanding of cometary physics, composition, and formation (Hendrix et al., 2020).

Remote observations of such exospheric emissions, continuously performed over time, provide a set of data that are pivotal for the study of the seasonal dynamics of the exosphere, allowing the understanding of the formation mechanisms and surface release processes that support the exosphere itself. A similar set of data can be obtained via in-situ instruments, which provide very precise measurements in terms of chemical composition, dynamics, and evolution (Mandt et al., 2012; Teolis et al., 2015). However, such in-situ measurements are always spatially and temporally limited and, in general, they are not suitable for detecting constituents having low concentrations, due to instrumental limitations and/or local contamination (Kammer et al., 2013; Koskinen et al., 2011). In contrast, UV imaging spectroscopy allows for large spatial coverage, denser temporal analysis, as well as measurements of the concentration of a large set of constituents not typically detectable with in-situ techniques.

In addition to the primary role of studying exospheres, EUV/FUV spectroscopy can provide complementary information in many other fields of planetary science. An example is the detection of surface water ice deposits, which can be identified through the H Lyman-α (i.e. λ = 121.6 nm) albedo drop-off measurements on perpetually shadowed craters and polar regions of celestial bodies devoid of collisional atmosphere (Hendrix and Hansen, 2008; Hendrix et al., 2012; Hayne et al., 2015). The EUV/FUV albedo measurement is also complementary to many geological studies of the surface via albedo measurements obtained by push-broom scans (Gladstone et al., 2012; Mandt et al., 2016). In particular, in the range between 150 – 300 nm, the albedo provides additional/complementary information on the geological nature and composition of the surface; for instance, pyroxenes, feldspars, olivines and chondritic meteorites show a valuable reduction of the albedo between 150 – 300 nm, which is not found in minerals containing valuable concentrations of iron, such as ilmenite, magnetite and others. A similar concept can be applied also to the observation of the integrated albedo of a rocky body, as recently made by BepiColombo/PHEBUS (Chaufray et al., 2023), or to a system of dust as in the case of Cassini/UVIS, which provided information on the structure, composition, and particle distribution of Saturn rings (Jarmak et al., 2022). Furthermore, the observation of extended comet comas at the H Ly-α allows the evaluation of the H atoms abundance, coming from a photo-dissociation of OH and H_2O

molecule, giving an indirect estimation of the water out-gassing rate of the comet (Yi et al., 2007).
Finally, among the secondary science objectives in which EUV/FUV spectroscopy can give valuable contributions, there is also the study of auroral phenomena on gas giants or magnetically active bodies. Cassini/UVIS observed the auroral footprint on Enceladus and Saturn, enabling the estimation of auroral electron energies(Gustin et al., 2017; Pryor et al., 2011). Similarly, Juno/UVS has observed auroral phenomena on Jupiter, providing insightful details on charged particle acceleration processes and their interaction with the magnetosphere (Gladstone et al., 2017). The achievement of primary and secondary scientific objectives through an EUV/FUV spectrometer involves the use of different observational modes, which depend on the specific target under investigation and the operational orbits. Figure 1 reports a general overview of such observational modes, highlighting the characteristics and the main scientific returns expected from each of these.

The development of FUV/EUV spectrometers operating with improved performance is crucial for the upcoming planetary exploration missions. The PLUS (PLanetary Ultraviolet Spectrometer) project, funded by the Italian Space Agency (ASI), has been conceived within this framework, with the aim of developing the technology to be used for a new generation of FUV/EUV spectrometers with high spatial and spectral resolution, improved detection limits, shorter observation integration time, and high dynamic range (Pelizzo et al., 2021a). Such objectives have been achieved by adopting an optical scheme based on two channels, each of which has a proper optical coating designed to maximize the reflectance. Additionally, a new concept of high dynamic-range and low-noise photon counting detectors based on a micro-channel plate (MCP) coupled with an Application-Specific Integrated Circuit (ASIC) readout system has been developed.

2. Instrument concept

PLUS project (Pelizzo et al., 2021a) was funded by ASI with the aim of developing the technologies needed for the realization of a high-performance dual-channel imaging spectrograph capable of operating in the spectral range between 55 nm to 200 nm. The main strategies followed to obtain an improvement in the instrument performance are:

a. the use of a new optical scheme based on less critical optical components;
b. a more careful division of the two spectral channels allowing a more effective optimization of the optical coatings, with a consequent beneficial increase in the effective area of the instrument;
c. the development of a new concept of MCP detector based on an ASIC readout system, with high dynamic range and photon counting capability.

2.1. Optical design:

PLUS is based on a multichannel FUV/EUV imaging spectrometer working in 55- 200 nm spectral range. The improvement with respect to previous solutions (Gladstone et al., 2005; Stern et al., 2005; Quémerais et al., 2020), is the use of a compact variable-line-spaced (VLS) grating configuration based on the Harada layout (Harada et al., 1991). In this configuration, the required aberration correction is achieved with a specific out-of-Roland geometry, which further optimizes the aberration compensation thanks to the use of two spherical VLS gratings. The first channel works in the EUV ($\lambda \simeq 55 - 120$ nm) whereas the second one in the FUV far ultraviolet ($\lambda \simeq 115 - 200$ nm); however, the second channel can be potentially extended up to 300 nm. With this division, each channel can be equipped with coatings having high efficiency in that restricted wavelength range, giving a higher effective area than previous solutions. For each channel, the design starts with the choice of the incidence angle, the number of lines per mm, and the curvature radius of the channel grating. Such three parameters are selected based on the available space for the

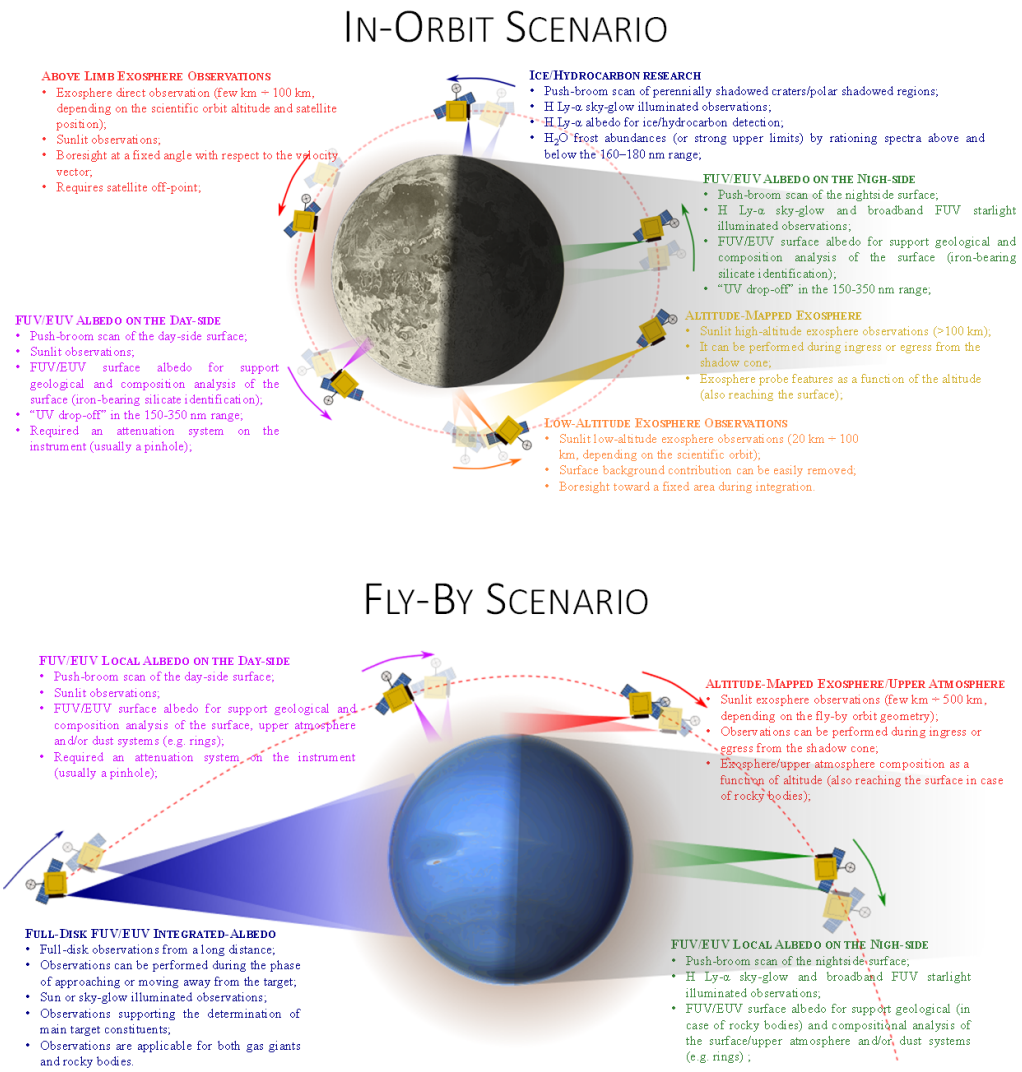

Fig. 1. Typical observational modes used for pursuing the scientific objectives with a FUV/EUV spectrometer.

spectrometer (i.e., incidence angle $\alpha + \alpha_G$ and the curvature radius R) and the target resolution (i.e., primary lines per mm d_0). After selecting these three parameters, the exit arm length of the grating (L_B), which determines the position of the detector, can be calculated. This computation is made by canceling the astigmatism term at the central wavelength of the channel being designed (i.e., the F_{02} term). The determination of the L_B arm establishes the magnification of the system, which automatically also identifies the slit width. By using a VSL grating, whose grooves density distribution is given by the relationship

$$n(w) = \frac{1}{d_0}\left(w + \frac{B}{R}w^2 + \frac{C}{R^2}w^3 + \frac{D}{R^3}w^4\right),$$

the coefficient B, C, and D can be computed to place the spectral focus at the detector plane (i.e. $F_{20} = 0$), and removing the spherical aberration and the coma (i.e. $F_{30} = 0$ and $F_{40} = 0$) for the channel central wavelength. With this design, residual aberrations, mainly astigmatism, are present at the edge wavelengths of the channel. Further partial compensation of such residual aberrations can be performed by slightly rotating the detector with an angle α_D. The collecting mirror of the spectrometer is an off-axis parabola working in a quasi-normal incidence configuration. Figure 2 shows the conceptual layout of the instrument. The best compact design obtained foresees a 40 mm diameter parabola, having $f = 170$ mm and working at 30° of incidence, a spectrometer entrance slit of 200 μm. The two channels adopt spherical VLS gratings, one having a curvature radius $R = 201.4$ mm and a central groove density of 2400 mm^{-1} and the other one a $R = 215.0$ mm central groove density of 1600 mm^{-1}. For this design, a SiC coating was considered for the EUV channel grating (Favaro et al., 2022) whereas a MgF_2-protected Al coating was selected for the FUV channel grating. Such coatings will be tested for stability in space environment (Pelizzo et al., 2011, 2018, 2021b). In this solution, the primary parabola is half area coated with SiC and the other half area coated with Al/MgF_2 to improve as much as possible the channel effective areas. Considering a detector pixel size of 35 μm, the best design shows a PSF at the central wavelength is comparable with the pixel size whereas at the edge wavelengths, the residual aberrations produce a PSF of 4 pixels along the spectral direction and 5 pixels along the spatial direction in the EUV channel; for the FUV channel, the PSF obtained for the edge wavelengths is slightly bigger, being of 5 pixels along the spectral direction and 6 pixels along the spatial direction. By considering an extended source that fulfills the width of the entrance slit and a height equal to the pixel size, the spectrometer shows a spectral resolution < 0.5 nm and a spatial resolution < 0.11° is expected for the EUV channel; for the FUV channel, a spectral resolution of < 0.6 nm and a spatial resolution < 0.18° is instead obtained. Based on the experience given by previous missions equipped with an EUV or FUV spectrometer, the scientific return typically requires a spectral resolution of at least 0.5 - 1 nm, depending on the specific observation. Normally, a good SNR in exosphere emission observations is already given by spectral resolutions of 0.5 nm or better whereas in occultations or albedo observations, a 1 nm spectral resolution is typically enough in most cases (Hansen et al., 2006; Byron et al., 2020; Steffl et al., 2020; Yoshikawa et al., 2014).

2.2. Detector:

MCPs are the most utilized detector for FUV/EUV applications (Vallerga et al., 2009), as they achieve the requirements of high efficiency in this wavelength range, high space and time resolution, solar blindness, photon counting capability and low dark count rate (Conti et al., 2022). The most part of space instruments developed so far use MCPs architecture based on either delay-line or resistive anode as read-out system. Some examples are the ALICE-class spectrometers (Stern et al., 2005) or PHEBUS (Yoshioka et al., 2012). In these cases, a high SNR and efficiency are achieved by using a stack of MCPs, at least three of them in cascade. However, the high gain obtained from such multiplication stages potentially leads to a reduction of the detector's lifetime. Moreover, this solution dramatically limits the dynamic range of the detector, reducing the performance in many cases, such as in the exospheres observation, where signal intensities with differences of several orders of magnitude coexist. Although the recent technologies in the MCPs production can help to extend the life of the detectors (Siegmund et al., 2013; Ertley et al., 2017), the use of a very low-noise read-out system is certainly one of the most promising solutions to reduce the MCP gain requirement, leading a consequent advantage for the dynamic-range and life-time. Following this philosophy, the PLUS MCP detector is based on an ASIC read-out system, called MIRA (MIcrochannel plate Readout ASIC), which implements the anode array, low noise front-end electronics chains ($rms \leq 30e^-$, thus allowing the use of an MCP gain lower than

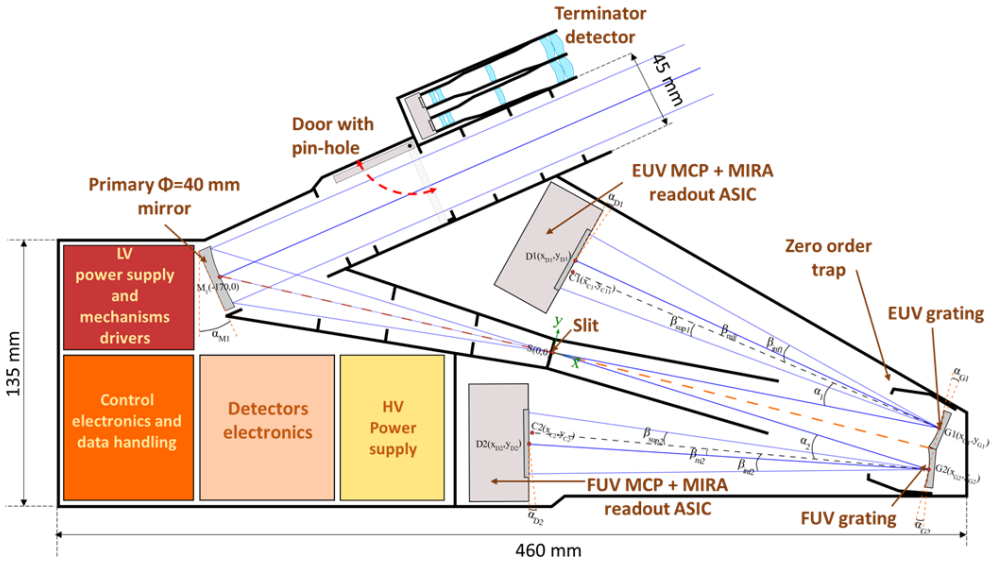

Fig. 2. PLUS optical layout

5000) and photon counting capability directly on chip. The chip can be also set in order to achieve a dynamic range at the order of 2000-3000, a typical value found between a generic ion emission line and the H_I Ly$-\alpha$ line during a direct sunlit exospheric observation. Figure 3 shows the architecture of the detector, where each pixel contains an anode to collect the electrons emitted by the MCP, a low noise amplifier and filter to maximize the SNR, a comparator to recognize and count single photon events, a logic to correct the charge sharing among pixels and two counters, which will form the counting matrix. To prevent dead-time, each pixel hosts two counters (C#1 and C#2), where one will be used for photon-counting, while the second for the readout (Fabbrica et al., 2022).

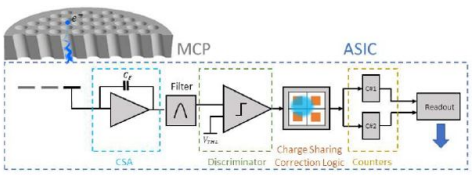

Fig. 3. Detector architecture

The spatial degradation is avoided through the Charge Control Logic circuit (CCLC) which identifies the pixel with the most collected charge, transfers all the adjacent pixel charges to the winner pixel, and avoids fake hits (see Figure 4). Three different modes of CCLC were implemented in MIRA, as described in Fabbrica et al. (2022). The philosophy of this detector can be easily extended to realizing detectors having a nominal matrix dimension of 1024×1024 pixels (Uslenghi et al., 2022).

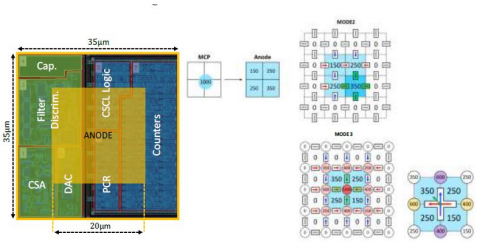

Fig. 4. Pixel electronic and Charge Sharing Logic

3. Instrument prototype:

A simplified prototype of the EUV channel based on a 1200 mm^{-1} grating has been realized. On the concave grating was deposited a SiC coating, achieving an efficiency of the order of 13.3% at 93 nm. The grating was mounted in a vacuum chamber, which represents the spectrograph demo (Figure 5). Within the project, a second grating coated by Al/MgF_2 was deposited as well, achieving a reflectance of 22.1% at 121.6 nm: this second grating is the main component for the FUV channel. The prototype has been tested in the Luxor laboratory in Padua, using a Hollow Cathode source with an EUV-CCD detector for the spectral calibration of the channel demonstrator and, then, with the MIRA-MCP demo for its testing (Figure 6). The spectral calibration was performed by using He, Ar and Ne gas on the Hollow Cathode lamp and determining the pixel-wavelength conversion. Moreover, based on the Ar and Ne spectra, the spectral resolution of the demo was estimated, founding a value of $\simeq$ 0.8 nm at the center of the spectral image and $\simeq$ 1.1 nm at the edge. Such values were expected for this simplified prototype.

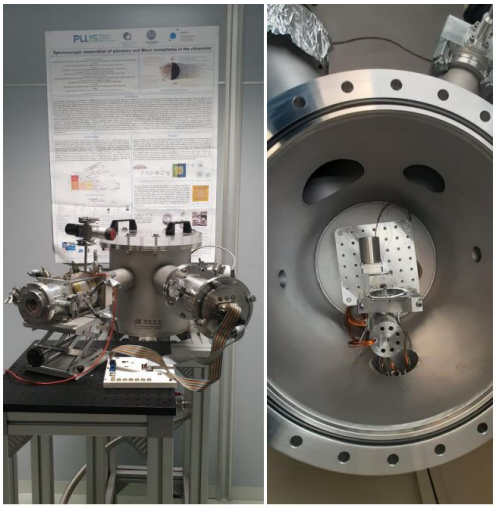

Fig. 5. EUV channel demonstrator in vacuum chamber; on the right: the EUV channel grating mounted on the support in the chamber

Fig. 6. Calibration activities: on the top panel the spetrograph prototype with the EUV CCD camera during spectral calibration; on the bottom panel the MIRA-MCP detector demo integrated on the spetrograph prototype.

Fig. 7. Integration of the detector in the mechanical support

The detector demonstrator was based on the MIRA and it implemented a MCP detector of 32(spectral)×32(spatial) pixels, with the pixel pitch of 35 μm (Fabbrica et al., 2024). Figure 7 shows the integration of the MIRA-MCP detector. The detector prototype has been tested in a vacuum chamber, with a pressure of $1 \cdot 10^{-6}$ mbar. The assembly was illuminated with a LED with emission peak at 245 nm, exploiting the residual efficiency of the bare

MCP at these wavelengths. The photon event footprints have been characterized as a function of the voltages applied to MCP and anode gap, using MIRA readout mode 1 (Uslenghi et al., 2024). In this mode all the pixel over threshold are counted and the CCLC is bypassed, thus, under an input photon flux low enough to avoid photon overlapping, the size of the photon events can be measured. Based on the results of these preliminary tests, the optimal set of voltages for MIRA operations have been evaluated and used in a subsequent linearity test, measuring the photons detected using MIRA standard readout mode (with CCLC) as a function of the incoming flux. Finally, after the integration of the MIRA-MCP detector demo with the simplified spetrograph prototype, the observation of the Ar doublet (i.e. at 92 nm and 93.2 nm) was successfully performed.

4. Conclusion

Space missions equipped with spectroscopic instruments operating in the extreme ultraviolet (EUV, $\lambda = 50 - 120$ nm) and in the far ultraviolet (FUV, $\lambda = 120 - 300$ nm) play a fundamental role in various scientific fields, such as in solar and in the study of planets and minor bodies. In particular, the development of FUV/EUV spectrometers operating with improved performance is crucial for the upcoming planetary missions. The PLUS (PLanetary Ultraviolet Spectrometer) project, funded by the Italian Space Agency (ASI), has been conceived with the aim of developing the technology to be used for a new generation of FUV/EUV spectrometers with high spatial and spectral resolution, improved detection limits, shorter integration time, and high dynamic range. In the project has been designed a new generation of spectrometers, based on two separate channels with specific optical coatings that maximize the efficiency of the instrument: the SiC coating for the EUV channel and the Al+MgF_2 for the FUV. The two channels adopt two spherical concave holographic variable line space gratings to minimize aberrations. The detector is an innovation with respect to the state of the art: it is an MCP coupled to an ASIC read-out system that extends both the lifetime and dynamic range of the detector; in this way, the instrument will be highly performing in terms of both spatial and spectral resolution, having high dynamics and low integration times.
In order to validate the instrument idea in terms of efficiency and the new concept of MCP detector, a demonstrator operating in the EUV range was built, using a detector prototype having 32 x 32 pixels.

Affiliations
[5] Università di Padova, Dipartimento di Ingegneria dell'Informazione, via Gradenigo 6B, 35128 Padova, Italy e-mail: mariaguglielmina.pelizzo@unipd.it

References

Byron, B., Retherford, K., Greathouse, T., Wyrick, D., Cahill, J., Hendrix, A., Raut, U., Mandt, K., and Denevi, B. (2020). Far-uv observations of lunar rayed craters with lro-lamp. *Journal of Geophysical Research: Planets*, 125(3):e2019JE006269.

Chaufray, J.-Y., Quémerais, E., Koutroumpa, D., Robidel, R., Leblanc, F., Reberac, A., Yoshikawa, I., Yoshioka, K., Murakami, G., Korablev, O., et al. (2023). The euv reflectance of mercury's surface measured by bepicolombo/phebus. *Journal of Geophysical Research: Planets*, 128(3):e2022JE007669.

Conti, L., Barnstedt, J., Diebold, S., Höltzli, M., Kalkuhl, C., Kappelmann, N., Rauch, T., Schanz, T., Stelzer, B., Stock, A., et al. (2022). A photon counting imaging detector for uv space missions. In *Space Telescopes and Instrumentation 2022: Ultraviolet to Gamma Ray*, volume 12181, pages 94–105. SPIE.

Elphic, R., Delory, G., Hine, B. P., Mahaffy, P., Horanyi, M., Colaprete, A., Benna, M., Noble, S., and Team, L. S. (2015). The lunar atmosphere and dust environment explorer mission. *The Lunar Atmosphere and Dust Environment Explorer Mission (LADEE)*, pages 3–25.

Ertley, C., Siegmund, O., Tremsin, A., Hull, J., O'Mahony, A., Craven, C., and Minot, M. (2017). Microchannel plate imaging detectors for high dynamic range applications. *IEEE Transactions on Nuclear Science*, PP:1–1.

Fabbrica, E., Carminati, M., Butta, D., Uslenghi, M., Fiorini, M., Corso, A., Pelizzo, M. G., and Fiorini, C. (2022). Design of mira, a low-noise pixelated asic for the readout of micro-channel plates. *Journal of Instrumentation*, 17:C01047.

Fabbrica, E., Nassi, L., Ciavarella-Ciavarella, A., Carminati, M., Uslenghi, M., Fiorini, M., Corso, A. J., Pelizzo, M. G., and Fiorini, C. (2024). Mira: a low-noise asic with 35 μm pixel pitch for the readout of microchannel plates. *IEEE Transactions on Nuclear Science*.

Favaro, G., Bazzan, M., Amato, A., Arciprete, F., Cesarini, E., Corso, A., De Matteis, F., Dao, T. H., Granata, M., Honrado-Benítez, C., Gutiérrez-Luna, N., Larruquert, J., Lorenzin, G., Lumaca, D., Maggioni, G., Magnozzi, M., Pelizzo, M. G., Placidi, E., Prosposito, P., and Puosi, F. (2022). Measurement and simulation of mechanical and optical properties of sputtered amorphous sic coatings. *Physical Review Applied*, 18.

Gladstone, G., Stern, S., Ennico, K., Olkin, C., Weaver, H., Young, L., Summers, M., Strobel, D., Hinson, D., Kammer, J., Parker, A., Steffl, A., Linscott, I., Parker, J., Cheng, A., Slater, D., Versteeg, M., Greathouse, T., Retherford, K., and Zirnstein, E. (2016). The atmosphere of pluto as observed by new horizons. *Science*, 351:aad8866–aad8866.

Gladstone, G., Stern, S., Retherford, K., Black, R., Scherrer, J., Slater, D., Stone, J., Feldman, P., and Crider, D. (2005). Lamp: the lyman alpha mapping project aboard the nasa lunar reconnaissance orbiter mission. *Proceedings of SPIE - The International Society for Optical Engineering*, 5906.

Gladstone, G., Versteeg, M., Greathouse, T., Hue, V., Davis, M., Gérard, J.-C., Grodent, D., Bonfond, B., Nichols, J., Wilson, R., Hospodarsky, G., Bolton, S., Levin, S., Connerney, J., Adriani, A., Kurth, W., Mauk, B., Valek, P., Mccomas, D., and Bagenal, F. (2017). Juno-uvs approach observations of jupiter's auroras: Juno-uvs jupiter approach observations. *Geophysical Research Letters*, 44.

Gladstone, G. R., Retherford, K. D., Egan, A. F., Kaufmann, D. E., Miles, P. F., Parker, J. W., Horvath, D., Rojas, P. M., Versteeg, M. H., Davis, M. W., et al. (2012). Far-ultraviolet reflectance properties of the moon's permanently shadowed regions. *Journal of Geophysical Research: Planets*, 117(E12).

Gustin, J., Grodent, D., Radioti, A., Pryor, W., Lamy, L., and Ajello, J. (2017). Statistical study of saturn's auroral electron properties with cassini/uvis fuv spectral images. *Icarus*, 284:264–283.

Hansen, C. J., Esposito, L., Stewart, A., Colwell, J., Hendrix, A., Pryor, W., Shemansky, D., and West, R. (2006). Enceladus' water vapor plume. *Science*, 311(5766):1422–1425.

Harada, T., Kita, T., Bowyer, S., and Hurwitz, M. (1991). Design of spherical varied line-space gratings for a high-resolution euv spectrometer. *Proceedings of SPIE - The International Society for Optical Engineering*.

Hayne, P. O., Hendrix, A., Sefton-Nash, E., Siegler, M. A., Lucey, P. G., Retherford, K. D., Williams, J.-P., Greenhagen, B. T., and Paige, D. A. (2015). Evidence for exposed water ice in the moon's south polar regions from lunar reconnaissance orbiter ultraviolet albedo and temperature measurements. *Icarus*, 255:58–69.

Hendrix, A. R., Becker, T. M., Bodewits, D., Bradley, E. T., Brooks, S., Byron, B., Cahill, J., Clarke, J., Feaga, L., Feldman, P., et al. (2020). Ultraviolet-based science in the solar system: Advances and next steps. *arXiv preprint arXiv:2007.14993*.

Hendrix, A. R. and Hansen, C. J. (2008). Ultraviolet observations of phoebe from the cassini uvis. *Icarus*, 193(2):323–333.

Hendrix, A. R., Retherford, K. D., Randall Gladstone, G., Hurley, D. M., Feldman, P. D., Egan, A. F., Kaufmann, D. E., Miles, P. F., Parker, J. W., Horvath,

D., et al. (2012). The lunar far-uv albedo: Indicator of hydration and weathering. *Journal of Geophysical Research: Planets*, 117(E12).

Hörst, S. (2017). Titan's atmosphere and climate. *Journal of Geophysical Research: Planets*, 122.

Jarmak, S., Becker, T., Colwell, J., Jerousek, R., and Esposito, L. (2022). Solar occultation observations of saturn's rings with cassini uvis. *Icarus*, 388:115237.

Kammer, J., Shemansky, D., Zhang, X., and Yung, Y. (2013). Composition of titan's upper atmosphere from cassini uvis euv stellar occultations. *Planetary and Space Science*, 88:86–92.

Koskinen, T., Yelle, R., Snowden, D., Lavvas, P., Sandel, B., Capalbo, F., Benilan, Y., and West, R. (2011). The mesosphere and lower thermosphere of titan revealed by cassini/uvis stellar occultations. *Icarus*, 216(2):507–534.

Mandt, K. E., Gell, D. A., Perry, M., Hunter Waite Jr, J., Crary, F. A., Young, D., Magee, B. A., Westlake, J. H., Cravens, T., Kasprzak, W., et al. (2012). Ion densities and composition of titan's upper atmosphere derived from the cassini ion neutral mass spectrometer: Analysis methods and comparison of measured ion densities to photochemical model simulations. *Journal of Geophysical Research: Planets*, 117(E10).

Mandt, K. E., Greathouse, T. K., Retherford, K. D., Gladstone, G. R., Jordan, A. P., Lemelin, M., Koeber, S. D., Bowman-Cisneros, E., Patterson, G. W., Robinson, M., et al. (2016). Lro-lamp detection of geologically young craters within lunar permanently shaded regions. *Icarus*, 273:114–120.

Pelizzo, M., Corso, A., Santi, G., Uslenghi, M., Fiorini, M., Incorvaia, S., Toso, G., Fabbrica, E., Carminati, M., Fiorini, C., et al. (2021a). The planetary extreme ultraviolet spectrometer project. In *Astronomical optics: Design, manufacture, and test of space and ground systems III*, volume 11820, pages 348–355. SPIE.

Pelizzo, M., Corso, A., Tessarolo, E., Bottger, R., Hubner, R., Napolitani, E., Bazzan, M., Rancan, M., Armelao, L., Jark, W., et al. (2018). Morphological and functional modifications of optical thin films for space applications irradiated with low-energy helium ions. *ACS applied materials & interfaces*, 10(40):34781–34791.

Pelizzo, M., Corso, A. J., Zuppella, P., Windt, D., Mattei, G., and Nicolosi, P. (2011). Stability of extreme ultraviolet multilayer coatings to low energy proton bombardment. *Optics Express*, 19(16):14838–14844.

Pelizzo, M. G., Corso, A. J., Santi, G., Hübner, R., Garoli, D., Doyle, D., Lubin, P., Cohen, A. N., Erlikhman, J., Favaro, G., et al. (2021b). Dependence of the damage in optical metal/dielectric coatings on the energy of ions in irradiation experiments for space qualification. *Scientific reports*, 11(1):3429.

Pryor, W. R., Rymer, A. M., Mitchell, D. G., Hill, T. W., Young, D. T., Saur, J., Jones, G. H., Jacobsen, S., Cowley, S. W., Mauk, B. H., et al. (2011). The auroral footprint of enceladus on saturn. *Nature*, 472(7343):331–333.

Quémerais, E., Koutroumpa, D., Lallement, R., Sandel, B. R., Robidel, R., Chaufray, J.-Y., Reberac, A., Leblanc, F., Yoshikawa, I., Yoshioka, K., et al. (2023). Observation of helium in mercury's exosphere by phebus on bepi-colombo. *Journal of Geophysical Research: Planets*, page e2023JE007743.

Quémerais, E., Chaufray, J.-Y., Koutroumpa, D., Leblanc, F., Reberac, A., Lustrement, B., Montaron, C., Mariscal, J.-F., Rouanet, N., Yoshikawa, I., Murakami, G., Yoshioka, K., Korablev, O., Belyaev, D., Pelizzo, M. G., Corso, A., and Zuppella, P. (2020). Phebus on bepi-colombo: Post-launch update and instrument performance. *Space Science Reviews*, 216.

Siegmund, O., Richner, N., Gunjala, G., McPhate, J., Tremsin, A., Frisch, H., Elam, J., Mane, A., Wagner, R., Craven, C., and Minot, M. (2013). Performance characteristics of atomic layer functionalized microchannel plates. *Proc SPIE*, 8859.

Steffl, A. J., Young, L. A., Strobel, D. F., Kammer, J. A., Evans, J. S., Stevens, M. H., Schindhelm, R. N., Parker, J. W., Stern, S. A., Weaver, H. A., et al. (2020). Pluto's ultraviolet spectrum, surface reflectance,

and airglow emissions. *The Astronomical Journal*, 159(6):274.

Stern, S., Scherrer, J., Slater, D., Gladstone, G., Dirks, G., Stone, J., Davis, M., Versteeg, M., and Siegmund, O. (2005). Alice: The ultraviolet imaging spectrograph aboard the new horizons pluto mission spacecraft. *Proceedings of SPIE - The International Society for Optical Engineering*, 5906.

Stevens, M., Evans, S., Lumpe, J., Westlake, J., Ajello, J., Bradley, E., and Esposito, L. (2015). Molecular nitrogen and methane density retrievals from cassini uvis dayglow observations of titan's upper atmosphere. *Icarus*, 247.

Teolis, B., Niemann, H., Waite, J., Gell, D., Perryman, R., Kasprzak, W., Mandt, K., Yelle, R., Lee, A., Pelletier, F., Miller, G., Young, D., Bell, J., Magee, B., Patrick, E., Grimes, J., Fletcher, G., and Vuitton, V. (2015). A revised sensitivity model for cassini inms: Results at titan. *Space Science Reviews*, 186:1–38.

Uslenghi, M., Faccini, D., Fiorini, M., Incorvaia, S., Toso, G., Schettini, L., Carminati, M., Fabbrica, E., Fiorini, C., Pelizzo, M. G., et al. (2022). Development of a novel photon counting detector for uv spectrographs. In *X-Ray, Optical, and Infrared Detectors for Astronomy X*, volume 12191, pages 841–850. SPIE.

Uslenghi, M., Toso, G., Schettini, L., Fiorini, M., Incorvaia, S., Nassi, L., Adele, C.-C., Carminati, M., Fiorini, C., Pelizzo, M. G., Padovani, M., Corso, A. J., and Meneguzzo, A. (2024). Preliminary characterization of a mcp photon counting detector prototype based on a custom-developed readout asic. *Proceedings of SPIE - The International Society for Optical Engineering, in press*.

Vallerga, J., McPhate, J., Tremsin, A., and Siegmund, O. (2009). The current and future capabilities of mcp based uv detectors. *Astrophysics and Space Science*, 320:247–250.

Yi, W., Park, J., and Lee, J. (2007). Photodissociation dynamics of water at lyman alpha (121.6 nm). *Chemical physics letters*, 439(1-3):46–49.

Yoshikawa, I., Yoshioka, K., Murakami, G., Yamazaki, A., Tsuchiya, F., Kagitani, M., Sakanoi, T., Terada, N., Kimura, T., Kuwabara, M., et al. (2014). Extreme ultraviolet radiation measurement for planetary atmospheres/magnetospheres from the earth-orbiting spacecraft (extreme ultraviolet spectroscope for exospheric dynamics: Exceed). *Space Science Reviews*, 184:237–258.

Yoshioka, K., Murakami, G., Yoshikawa, I., Maria, J.-L., Mariscal, J.-F., Rouanet, N., Mine, P.-O., and Quémerais, E. (2012). Optical performance of phebus/euv detector onboard bepicolombo. *Advances in Space Research*, 49:1265–1270.